Sensors and Actuators: A. Physical 332 (2021) 113204

Contents lists available at ScienceDirect

Sensors and Actuators: A. Physical

journal homepage: www.elsevier.com/locate/sna

Paper-supported WS_2 strain gauges

Wenliang Zhang[a], Riccardo Frisenda[a], Qinghua Zhao[a,b,c], Felix Carrascoso[a], Abdullah M. Al-Enizi[d], Ayman Nafady[d], Andres Castellanos-Gomez[a,*]

[a] Materials Science Factory, Instituto de Ciencia de Materiales de Madrid (ICMM-CSIC), Madrid E-28049, Spain
[b] State Key Laboratory of Solidification Processing, Northwestern Polytechnical University, Xi'an 710072, PR China
[c] Key Laboratory of Radiation Detection Materials and Devices, Ministry of Industry and Information Technology, Xi'an 710072, PR China
[d] Department of Chemistry, College of Science, King Saud University, Riyadh 11451, Saudi Arabia

ARTICLE INFO

Article history:
Received 15 July 2021
Received in revised form 15 October 2021
Accepted 1 November 2021
Available online 10 November 2021

Keywords:
Strain gauge
Tungsten disulfide (WS2)
Paper-based electronics
Strain Sensor
Disposable electronics
Mass sensor

ABSTRACT

Environmentally friendly and low-cost sensors are needed for the next generation disposable electronics applications. Given its low-cost, availability and biodegradability, paper-based devices are a very promising. Here we demonstrate the fabrication of a tungsten disulphide (WS_2) strain sensor on standard copy paper. The WS_2 is deposited through direct abrasion of WS_2 powder against the paper surface making the fabrication of the device low-tech and cost effective. The fabricated strain gauge devices present gauge factors up to ~70 for strains in the ± 0.5% range. These values are ~ 9 times larger than that obtained on devices with the same geometry but using a graphite film instead a WS_2 as a sensitive material. We demonstrate the potential of these WS_2-on-paper strain gauges by integrating them directly on a paper cantilever to sense mass and forces. We show how this very simple device can detect sub-milligram masses. Moreover, we also demonstrate the capability of transducing motion in mechanical resonators by gluing a WS_2-on-paper strain gauge on their surface.

Ubiquitous electronics applications like Internet of things, wearables or smart patches/tags will come together with an exponential growth of the electronic component production, eventually leading to an urgent problem of electronic waste handling [1–3]. In fact, only a very small fraction of standard silicon-based electronic components can be recycled thus motivating the exploration of alternative, eco-friendlier, substrate materials for electronic components. Although silicon will be still necessary in applications where a high level of electronic components integration is crucial, in other applications (like sensors) using alternative substrate materials could be easily achieved in the short term.

Among the different biodegradable substrate materials, paper has attracted the interest of the materials science community because of its ultra-low cost and availability [4–7]. Fabrication of electronic devices on paper substrates is, however, very challenging. In fact, paper is rough, fibrous and permeable which hampers the use of conventional lithographic techniques to fabricate electronic components. Up to now, most approaches are based on integrating electronic materials on paper substrates through inkjet printing [8–13]. Nonetheless, specialized paper surface treatments (that increase the price ~10 times and hamper its biodegradability) are required to print electronic components on paper. Recently, we demonstrated the integration of different van der Waals materials on standard printer/copy paper (untreated) through direct abrasion of powders of van der Waals materials against the rough surface of paper [14–18]. This deposition process is similar to drawing/writing with a pencil on paper: the friction force generated when a van der Waals material is rubbed against paper cleaves the crystals leading to a network of interconnected platelets.

Here, we demonstrate the fabrication of strain sensors on standard copy paper substrates using abrasion-induced deposited WS_2 films as sensing material. We obtained gauge factors up to ~70 for strains in the ± 0.5% range, a factor 9–10 times larger than that measured using graphite based paper-supported strain gauges. We illustrate the potential of these WS_2-on-paper strain gauges by fabricating a simple force/mass sensor and by transducing motion of mechanical resonators.

As shown in Fig. 1a, the paper-supported strain sensor devices are fabricated by abrasion induced deposition of WS_2 onto standard copy paper [15–17]. Briefly, the outline of the device channel and electrodes is printed out in a piece of standard copy paper (80 g/m^2) with an office laser printer. Then, Post-It tape is used to create a stencil to delimit the channel area and micronized WS_2 powder (0.6 µm APS Micronised WS_2, HAGEN Automation ltd.) is rubbed

* Corresponding author.
E-mail address: Andres.castellanos@csic.es (A. Castellanos-Gomez).

https://doi.org/10.1016/j.sna.2021.113204
0924-4247/

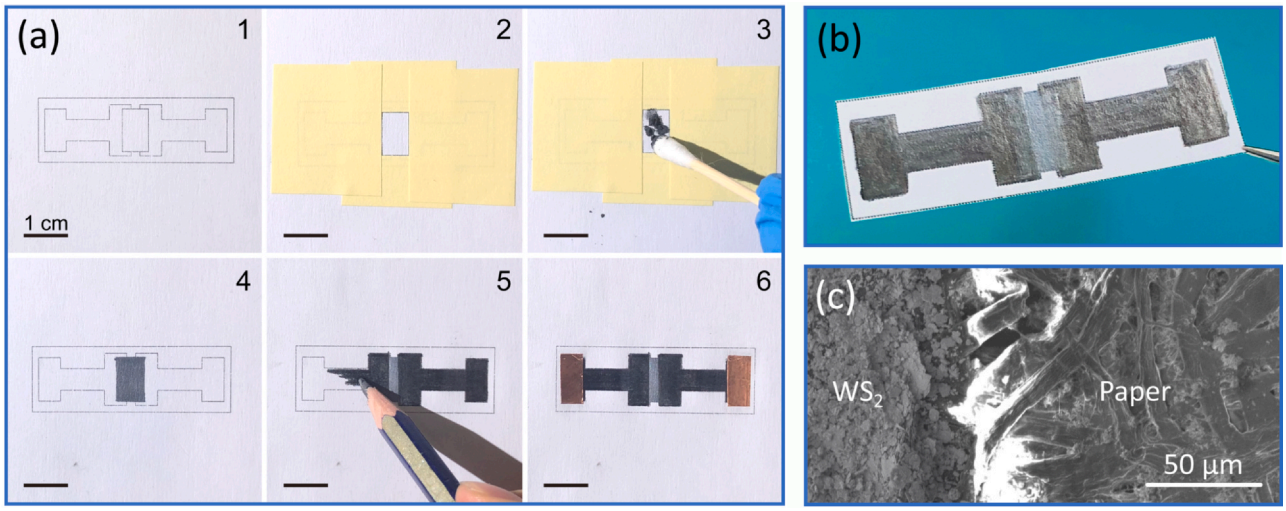

Fig. 1. WS_2-on-paper strain sensors. (a) Steps in the fabrication of the WS_2-on-paper strain sensors. (a.1) The outline of the device is printed on standard copy paper with an office laser printer. (a.2) The channel area is masked using Post-It tape. (a.3) WS_2 powder is rubbed against the unmasked paper with a cotton swab and the mask is removed (a.4). (a.5) Graphite electrodes are deposited onto the WS_2 channel by directly drawing with a 4B pencil. (a.6) Copper tape is attached to the graphite leads to allow soldering electrical connections. (b) Higher magnification picture of one device. (c) False colored scanning electron microscopy image of the paper covered with WS_2-bare paper interface.

against the surface of copy paper with a cotton swab to deposit the channel. The continuity of the film is tested with a handheld multimeter and the rubbing process is repeated until reaching a resistance between two probes separated by ~1–2 mm in the ~1–5 MΩ range. This relatively large resistance values span is due to the percolation nature of the electrical transport in the WS_2 films, as demonstrated from the statistical analysis of more than 100 WS_2 devices in Ref [17]. After that, the stencil is removed and graphite electrodes are deposited by direct drawing with a 4B pencil (~80% graphite content [19]) onto the WS_2 and paper surfaces following the printed electrode outline contour. This handcrafted device fabrication technique can limit their implementation in industrial applications. However, Nutting et al. recently implemented a system based on computer numerical control (CNC) to automatize a similar abrasion deposition technique, to deposit van der Waals materials on plastic substrates, opening a route for the scalability of this method [14].

Fig. 1b shows a picture of one of the WS_2 strain sensors fabricated on standard copy paper. A very comprehensive characterization of the morphology, chemical composition, electrical and optical properties of abrasion-induced deposited WS_2 films on copy paper can be found in Ref [17]. and we address the reader to that work for further details. Fig. 1c shows a scanning electron microscopy (SEM) image of the interface between the bare, uncovered, paper substrate and the deposited WS_2 film. On the paper substrate one can readily resolve the fibrous structure, due to the cellulose fibers composing the substrate. The WS_2 film covers the surface of the paper, filling in the gaps between the cellulose fibers, and creating a compact film of interconnected flakes.

To characterize the suitability of these devices in strain sensing applications we load the fabricated devices into a home-built three-points bending jig apparatus (see the inset in Fig. 2a) [20]. The devices are subjected to well-defined strains while the electronic transport characteristics are determined. Fig. 2a shows current *vs.* voltage characteristics (*IV*s hereafter) acquired at different levels of uniaxial strain, including tensile strain (positive strain values) and compressive strain (negative strain values). The resistance of the device changes monotonically when uniaxial strain is applied, as indicated by the change in slope of the *IV*s. For tensile strains the resistance increases while for compressive strains the resistance decreases. We attribute this behavior mostly to the sliding of flakes within the film rather than stretching/compressing of the individual WS_2 flakes [21,22]. In fact, as these films are formed by interconnected WS_2 flakes that interact to each other through van der Waals forces the flake-to-flake friction forces are very small and thus flake sliding is expected to occurs even when moderate stress is applied [23,24]. Upon tensile strain, the flakes slide apart reducing the flake-to-flake overlap and thus explaining the observed increase in the resistance. On the contrary, compressive strain makes flakes to slide towards a more compact configuration, increasing the overlap between flakes and reducing the resistance. The overall dependence of the device resistance on the applied strain can be better resolved in Fig. 2b where the relative change in resistance (with respect to the resistance at 0% strain, R_0) is displayed for different strain levels. The gauge factor (GF) or strain factor of the WS_2 paper-supported strain gauge device can be defined as:

$$GF = (\Delta R/R_0)/\varepsilon$$

where ε is the strain and ΔR is the difference between the resistance when subjected to a certain strain and R_0. The gauge factor is a very suitable figure-of-merit that allows to directly compare the performance of different strain sensors. In the WS_2-on-paper strain gauge shown in Fig. 2b we obtain a gauge factor of ~60 for tensile strain and ~40 for compressive strain. For comparison (Table 1), state-of-the-art metallic thin-film based strain gauges have gauge factors in the 2–10 range [25]. Recently, other paper-supported strain sensors, based on black phosphorus, ITO inks and carbon black, have been reported with gauge factors in the 4–40 range [26–28]. Graphite and graphene strain sensors on paper have been also demonstrated but the gauge factors span over a very broad range of values, 3–800 [29–32]. The reason for such a large variation in gauge factor of graphite/graphene based strain sensors in different reports is unclear. We thus decided to carry out a benchmarking test with graphite-based strain sensors fabricated and tested with the exact same protocol as the WS_2 sensors. Fig. 2c shows the measured relative change in device resistance as a function of strain, measured for 17 WS_2 and 12 graphite (4B pencil, ~80% graphite content [19]) devices. One can observe that the WS_2 devices show a stronger resistance change upon straining as compared with the graphite devices. The Supporting Information shows datasets for 5 different WS_2 devices and one graphite (4B) device for comparison. We have also tested graphite devices fabricated out of pure nano-graphite powder (MKN-CG-50, Lower Friction, MK IMPEX CORP) obtaining a similar behavior than that of 4B pencil based devices, we address the reader

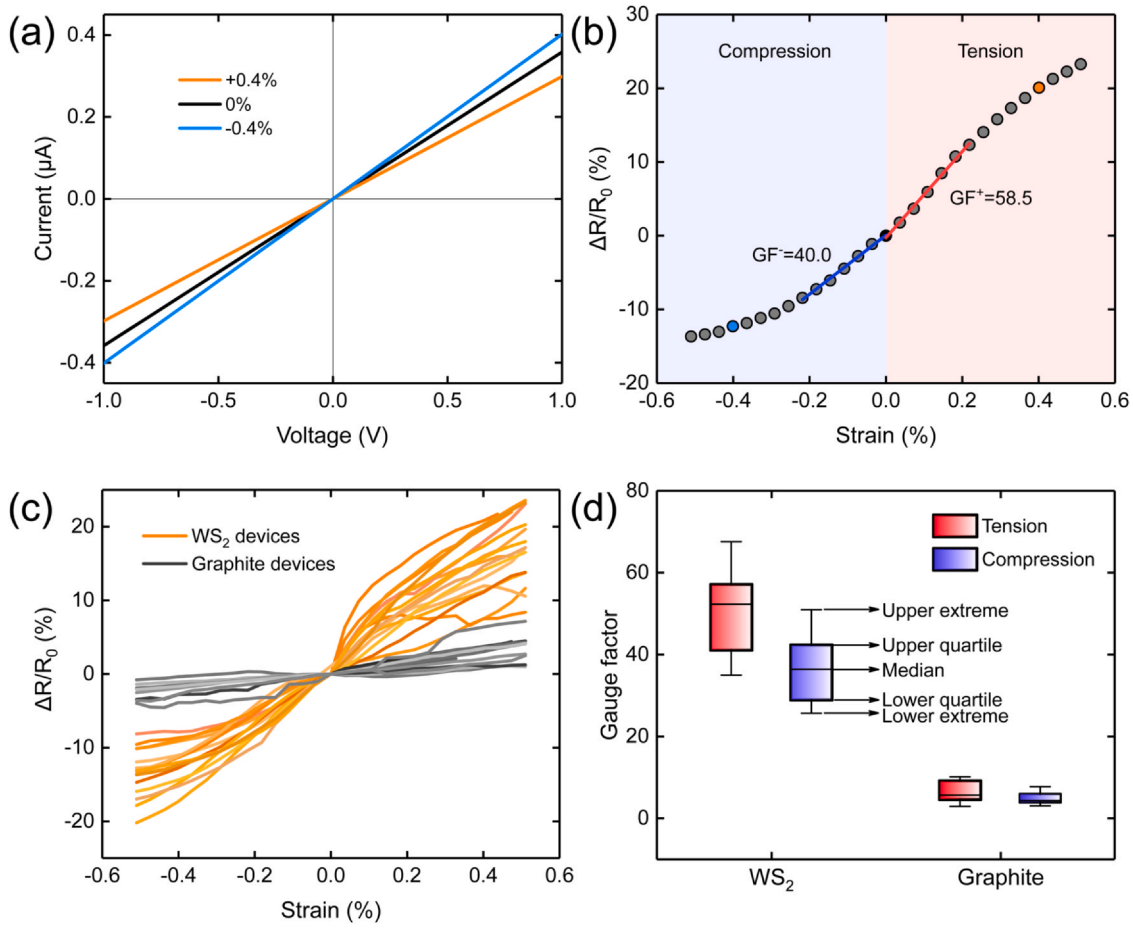

Fig. 2. Strain dependent resistance of WS_2-on-paper devices. (a) Current *vs.* voltage characteristics of a paper supported WS_2 strain gauge device, measured for different uniaxial strains. (Inset) Picture of the device loaded in a three-point bending jig apparatus to apply controllable strains. (b) Resistance changes as a function of the applied strain. The gauge factor (GF) can be extracted from the slope of the curve. (c) Comparison between the strain dependent resistance changes measured on 17 WS_2 devices and that measured on 12 devices with graphite sensing channel. (d) Box plot summarizing the gauge factors measured, within ± 0.2% strain range, for the WS_2- and graphite-based devices.

Table 1
Summary of gauge factor values reported for other conventional and paper-supported strain gauges. The table indicates the strain sensitive material used, the substrate, the method to deposit the sensing material and the reported gauge factor. Gauge factor values highlighted with ^{t} or ^{c} indicate values obtained upon tensile or compressive strains, respectively.

Sensing material	Substrate	Method	Gauge factor	Ref.
Metallic thin-film	Flexible polymer (usually Kapton)	Lithography + metal deposition	2–10	[25]
Black phosphorus	Paper	Sonochemistry, hydrothermal	6.1	[26]
Carbon black	Paper	Dip-coating	4.3	[27]
ITO nanoparticles	Paper	Hand-painting	41.98^t; 21.36^c	[28]
Graphite glue	Paper	Stencil printing	804.9^t; 142.1^c	[29]
Water-based graphene inks	Paper	Inkjet-printing	125	[30]
Graphite pencil-trace (HB)	Paper	Drawing	26	[31]
Graphite pencil-trace (2B)	Paper	Drawing	536.6	[32]
Graphite pencil-trace (2B)	Paper	Drawing	34	[34]
Carbon black/carbon nanotube (CB/CNT)	Paper	Dip-coating	7.5^t; 2.6^c	[35]
Molybdenum carbide-graphene (MCG) composites	Paper	Direct laser writing	73^t; 43^c	[36]
Reduced graphene oxide (rGO)	Paper	Drop-casting	66.6 ± 5	[37]
Graphite	Hybrid graphite-paper	Preparation of graphite infiltrated paper	27	[38]
Graphene	Mulberry paper	Meyer-rod coating	3.82	[39]
Carbon paper	Carbon paper	Pyrolysis	25.3	[40]
Carbonized crepe paper	Carbonized crepe paper	Pyrolysis	10.10	[41]
Laser-fabricated graphitic platelets	Polyimide (PI)/paper	Direct laser writing	13	[42]
Au nanoparticles	Abrasive paper	Direct-current (DC) sputtering	75.8^t; 10.7^c	[43]
Single-layer graphene	PDMS	Chemical vapor deposition (CVD), photolithography	42.2	[44]
WS_2	PET	Atomized spray casting deposition	14	[45]
WS_2	Paper	Direct abrasion	67.6^t; 51.0^c	This work
Graphite (4B)	Paper	Direct abrasion	10.2^t; 7.8^c	This work
Graphite (nanographite)	Paper	Direct abrasion	9.5^t; 11.1^c	This work

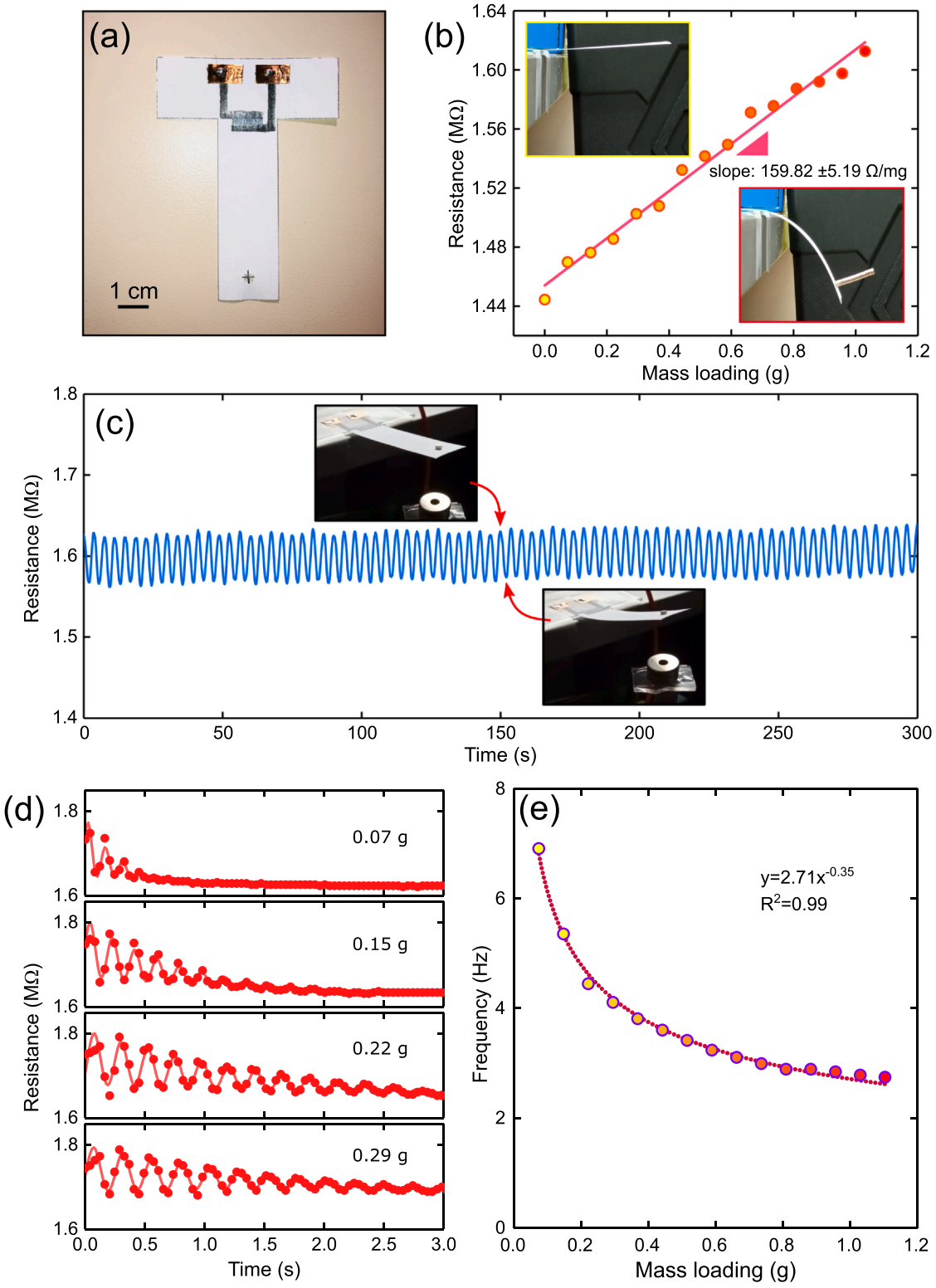

Fig. 3. Paper-based cantilever with integrated WS_2 strain gauge. (a) Picture of the paper cantilever with a WS_2 film strain gauge integrated at the base of the cantilever. (b) Resistance of the strain gauge as a function of the mass load. (Insets) Pictures of the cantilever: unload (top left) and loaded with ~1.0 g (bottom right). (c) Resistance of the WS_2 film *vs.* time while the paper cantilever is subjected to ~80 cycles of bending/releasing. (d) Resistance of the WS_2 film *vs.* time acquired when the paper cantilever, loaded with different test masses, is mechanically excited to induce a ring-down. The datapoints have been fitted to a damped harmonic oscillator model to extract the resonance frequency of the cantilever. (e) Resonance frequency of the cantilever measured for different mass loading conditions.

to the Fig. S3 to see the results. From the slope at low strain values one can quantitatively extract the gauge factor of the different devices. Fig. 2d presents the statistical summary of the results in a box-plot. Our graphite devices show gauge factors with a median value of 5.7 (for tensile strain) that are compatible with the lower bound of the reported values in the literature for graphite/graphene strain sensors on paper. On the other hand, WS_2-on-paper devices show gauge factor values up to 67.6, ~9–10 times larger than that of

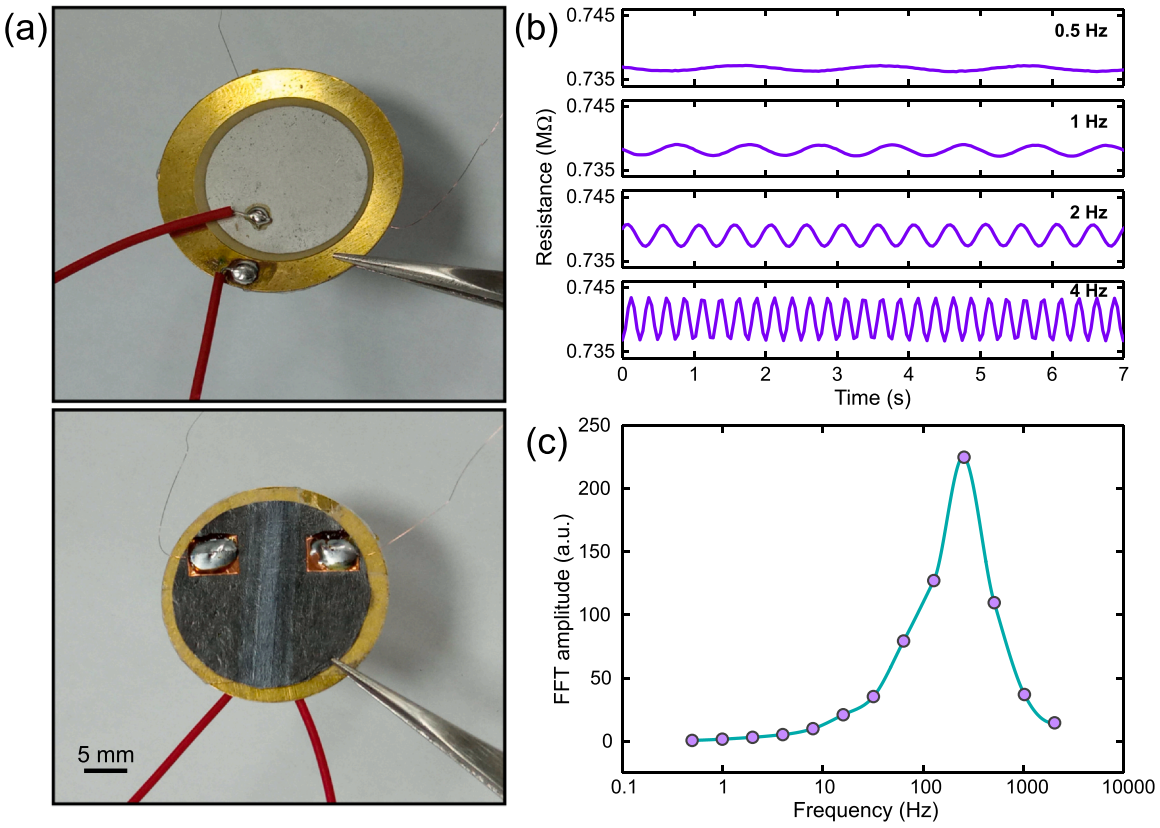

Fig. 4. Use of WS_2 strain gauge as a motion transducer. (a) Pictures of a piezoelectric disc buzzer (top) with a WS_2-on-paper strain gauge glued on its back side (bottom). (b) Resistance of the WS_2 film *vs.* time measured when the piezoelectric buzzer is excited with a sine wave of 0.5 Hz, 1 Hz, 2 Hz and 4 Hz (10 V_{pp}), respectively. (c) FFT amplitudes at various excitation frequencies.

graphite. We attribute the device-to-device variation shown in Fig. 2c to the percolative nature of the WS_2 film [33] that introduces an intrinsic variability between devices as the conduction paths through a percolative network are randomly distributed.

In order to illustrate the potential of the WS_2-on-paper strain sensors we have fabricated paper-based force and mass sensors that use a WS_2 strain gauge as transducer. The force/mass sensor is based on a cantilever made of copy paper and we fabricated a WS_2 strain gauge on its base to convert the deflections of the cantilever into an electrical signal (see Fig. 3a). We first test the use of such device to sense mass by loading the cantilever free end with test-masses and measuring the change in resistance (Fig. 3b). Upon mass loading, the cantilever deflects downwards (see insets in Fig. 3b) creating a tensile strain on the base of the cantilever that can be detected with the WS_2 strain gauge integrated directly on the surface of the paper cantilever. The resistance of the device raises gradually with increasing mass loading, and one can obtain a slope of ~160 Ω/mg that represents the mass sensitivity of the sensor.

In order to test the reproducibility of this sensor we have subjected it to 80 deflection cycles by gluing a magnet at the free end of the cantilever and mounting another magnet on a motorized stage to deflect the cantilever through magnetic force repulsion. Fig. 3c presents the resistance changes during these deflection cycles, showing how the device responds fast to the deflection change and with a good reproducibility, with an overall drift of less than 0.8% in the 5 min measurement. We address the reader to the Fig. S4 to see a long-term test with nearly 600 loading/unloading cycles. In such long-term measurement one can see an overall slow drift of the current value. The drift is about 7% per hour (in good agreement with the drift observed in the short-term measurement) and we attribute it to temperature or humidity changes. Indeed, we have recently observed that changes in temperature in the order of few degrees can induce changes in the WS_2 resistance of up to ~10–20% [16]. Nonetheless, the strain-induced resistance modulation, due to the strain/release cycles, remains rather stable over long periods of time (~1.5 h). Therefore, even though temperature and humidity changes can alter the resistance baseline of the device the strain-induced resistance change is robust.

An alternative way of sensing mass with this device is to use the WS_2 strain gauge to study the dynamics of the paper cantilever. Fig. 3d shows the resistance of the WS_2 film as a function of time for a cantilever loaded with 1–4 test masses (73.6 mg each test mass) when it is mechanically excited. One can observe that the current oscillates in time and its amplitude decays, as expected for a damped harmonic oscillator. One can fit the measured resistance *vs.* time traces to a damped oscillator to accurately extract the resonance frequency of the paper cantilever, that decreases monotonically upon mass loading (see Fig. 3e). Therefore, one can determine the mass load alternatively to the direct resistance change measurement from the determination of the resonance frequency of the cantilever. For low mass load, the change in frequency is in the order of 20 mHz/mg and thus one could easily resolve sub-mg test masses.

The capability of the WS_2-on-paper strain gauges to transduce strain dynamically (Fig. 3e) motivated us to test the performance of these devices to transduce the motion of mechanical resonators by directly sticking a paper with a WS_2 strain gauge on the surface of the mechanical resonator. Fig. 4a shows pictures of a WS_2-on-paper strain sensor glued on the backside of a piezo-buzzer disc. The piezo-buzzer is then excited by sending a sine wave signal to the piezoelectric material with a function waveform generator (Tenma 72–14110) and the resistance of the WS_2-on-paper strain gauge is measured. Fig. 4b shows the resistance of the WS_2 strain gauge as a function of time when the piezo-buzzer is excited with sine waves of frequencies 0.5 Hz, 1 Hz, 2 Hz and 4 Hz. One can see how the

resistance of the WS_2 strain gauge oscillates following a sine wave of the same frequency as the piezo-buzzer excitation, indicating that the motion of the piezo-buzzer induces a strain on the WS_2-on-paper that is transduced as a change in resistance. By repeating the experiment at different piezo-buzzer excitation frequencies one can get information about the mechanical resonances of the piezo-buzzer disc (Fig. 4**c**). In this example the disc has a broad resonance around 256 Hz. Interestingly, the paper-based strain gauge could be used to transduce the motion of the piezo-buzzer up to 2 kHz (the upper frequency limitation of our electrical measurement system) and thus the response time of the WS_2-on-paper strain gauge is < 0.5 ms.

1. Conclusions

In summary, we fabricated strain sensors on standard copy paper substrates integrating a WS_2 film, as sensing material, contacted with graphite electrodes. The WS_2 was deposited through a low tech and cost effective all-dry abrasion-induced deposition method that does not require of any specialized fabrication instrumentation. The graphite electrodes were directly drawn onto the WS_2 film using a high-graphite content pencil (B-type). The resistance of the strain sensors strongly depends on the applied strain, reaching gauge factor values up to ~70, 9–10 times larger than the values obtained when a graphite film is used. We demonstrate the direct integration of the WS_2-on-paper strain sensor on a paper cantilever, allowing for the transduction of cantilever deflection, allowing for mass and force sensing. We demonstrate a mass sensitivity of ~160 Ω/mg using this simple disposable mass sensor. We have also demonstrated how gluing these paper-based sensors to a mechanical resonator we can transduce its motion even at frequencies > 2 kHz. The results presented here open the door to the integration of other van der Waals materials in the fabrication of biodegradable, low-cost and disposable paper-supported strain sensors.

2. Materials and methods

2.1. Materials

Standard (untreated) copy printer paper (80 g/m^2) were used as supporting substrates because their low cost and availability. Tungsten disulfide (WS_2) from HAGEN automation Ltd. (0.6 µm APS Ultra Grade Micronised) was used as sensing channel material. Graphite pencil (4B, Faber Castell) was used to pattern graphite-based electrical leads to connect the WS_2 channel to the readout electronics. Nano-graphite powder with the average particle size of 50 nm (PN: MKN-CG-50) was purchased at Lowerfriction Lubricants.

2.2. SEM and EDX

Scanning electron microscopy (SEM) and energy dispersive X-ray spectroscopy (EDX), using a FE-SEM, FEI Nova NANOSEM 230, was used to characterize the morphology and the composition of the WS_2 films deposited on paper. An electron energy of 7 keV were used for imaging and 14 keV for EDX spectroscopy.

2.3. Electrical measurements

Electrical measurements were carried out with a Keithley 2450 source measure unit. The WS_2-on-paper devices were fixed on a home-made three-points bending setup to conduct the well-defined tension and compression deformations. The electrical resistance of the device was determined by measuring current *vs.* voltage characteristics at various uniaxial strains. The variation of electrical resistance of the strain sensor was monitored with a fixed voltage of 1 V.

Funding sources

European Research Council through the project 755655, Ministry of Science and Innovation (Spain) through the project PID2020–115566RB-I00, Spanish Ministry of Economy, Industry and Competitiveness (Spain) through the fellowship FJCI-2017–32919, King Saud University through the Distinguished Scientist Fellowship Program (DSFP), China Scholarship Council through the grants 201908610178, 201706290035.

Supporting Information

Supplementary Information includes: extra datasets of some WS_2-on-paper strain gauge devices, electrical characteristics of a pencil-on-paper strain gauge upon strain, electrical characteristics of several nanographite-on-paper strain gauge upon strain.

Declaration of Competing Interest

The authors declare that they have no known competing financial interests or personal relationships that could have appeared to influence the work reported in this paper.

Acknowledgments

This project has received funding from the European Research Council (ERC, European Union) under the European Union's Horizon 2020 research and innovation program (grant agreement n° 755655, ERC-StG 2017 project 2D-TOPSENSE) and the Ministry of Science and Innovation (Spain) through the project PID2020–115566RB-I00. The authors extend their sincere appreciation to the Distinguished Scientist Fellowship Program (DSFP) at King Saud University (Saudi Arabia) for funding of this work. R.F. acknowledges the support from the Spanish Ministry of Economy, Industry and Competitiveness (MINECO, Spain) through a Juan de la Cierva-formación fellowship 2017 FJCI-2017–32919. W. Zhang acknowledges the grant from China Scholarship Council (CSC, China) under No. 201908610178. Q.H.Z. acknowledges the grant from China Scholarship Council (CSC, China) under No. 201706290035.

Appendix A. Supporting information

Supplementary data associated with this article can be found in the online version at doi:10.1016/j.sna.2021.113204.

References

[1] S.R. Forrest, The path to ubiquitous and low-cost organic electronic appliances on plastic, Nature 428 (2004) 911–918, https://doi.org/10.1038/nature02498
[2] C. Liang, Y. Li, J. Luo, Flexible electronics: the next ubiquitous platform, Proc. IEEE 100 (2012) 1486–1517, https://doi.org/10.1109/JPROC.2012.2190168
[3] V. Forti, C.P. Baldé, R. Kuehr, G. Bel, Global E-waste Monitor, 2020. Available online: ⟨https://www.itu.int/en/ITU-D/Environment/Documents/Toolbox/GEM_2020_def.pdf⟩.
[4] F. Eder, H. Klauk, M. Halik, U. Zschieschang, G. Schmid, C. Dehm, Organic electronics on paper, Appl. Phys. Lett. 84 (2004) 2673–2675, https://doi.org/10.1063/1.1690870
[5] A. Russo, B.Y. Ahn, J.J. Adams, E.B. Duoss, J.T. Bernhard, J.A. Lewis, Pen-on-paper flexible electronics, Adv. Mater. 23 (2011) 3426–3430.
[6] Y. Xu, G. Zhao, L. Zhu, Q. Fei, Z. Zhang, Z. Chen, F. An, Y. Chen, Y. Ling, P. Guo, S. Ding, G. Huang, P.Y. Chen, Q. Cao, Z. Yan, Pencil–paper on-skin electronics, Proc. Natl. Acad. Sci. 117 (2020) 202008422–202018301, https://doi.org/10.1073/pnas.2008422117
[7] D. Tobjörk, R. Österbacka, Paper electronics, Adv. Mater. 23 (2011) 1935–1961, https://doi.org/10.1002/adma.201004692
[8] J. George, A. Abdelghani, P. Bahoumina, O. Tantot, D. Baillargeat, K. Frigui, S. Bila, H. Hallil, C. Dejous, CNT-based inkjet-printed RF gas sensor: modification of substrate properties during the fabrication process, Sensors 19 (2019) 1768, https://doi.org/10.3390/s19081768
[9] A. Quddious, S. Yang, M. Khan, F. Tahir, A. Shamim, K. Salama, H. Cheema, Disposable, paper-based, inkjet-printed humidity and H2S gas sensor for passive sensing applications, Sensors 16 (2016) 2073, https://doi.org/10.3390/s16122073

[10] S. Kim, B. Cook, T. Le, J. Cooper, H. Lee, V. Lakafosis, R. Vyas, R. Moro, M. Bozzi, A. Georgiadis, A. Collado, M.M. Tentzeris, Inkjet-printed antennas, sensors and circuits on paper substrate, IET Microw., Antennas Propag. 7 (2013) 858–868, https://doi.org/10.1049/iet-map.2012.0685
[11] J. Sarfraz, A. Määttänen, P. Ihalainen, M. Keppeler, M. Lindén, J. Peltonen, Printed copper acetate based H2S sensor on paper substrate, Sens. Actuators B Chem. 173 (2012) 868–873, https://doi.org/10.1016/j.snb.2012.08.008
[12] J. Sarfraz, D. Tobjork, R. Osterbacka, M. Linden, Low-cost hydrogen sulfide gas sensor on paper substrates: fabrication and demonstration, IEEE Sens. J. 12 (2012) 1973–1978, https://doi.org/10.1109/JSEN.2011.2181498
[13] S. Conti, L. Pimpolari, G. Calabrese, R. Worsley, S. Majee, D.K. Polyushkin, M. Paur, S. Pace, D.H. Keum, F. Fabbri, G. Iannaccone, M. Macucci, C. Coletti, T. Mueller, C. Casiraghi, G. Fiori, Low-voltage 2D materials-based printed field-effect transistors for integrated digital and analog electronics on paper, Nat. Commun. 11 (2020) 3566, https://doi.org/10.1038/s41467-020-17297-z
[14] D. Nutting, J.F. Felix, E. Tillotson, D.-W. Shin, A. De Sanctis, H. Chang, N. Cole, S. Russo, A. Woodgate, I. Leontis, H.A. Fernández, M.F. Craciun, S.J. Haigh, F. Withers, Heterostructures formed through abraded van der Waals materials, Nat. Commun. 11 (2020) 3047, https://doi.org/10.1038/s41467-020-16717-4
[15] A. Mazaheri, M. Lee, H.S.J. van der Zant, R. Frisenda, A. Castellanos-Gomez, M. Lee, H.S.J. van der Zant, R. Frisenda, A. Castellanos-Gomez, MoS 2 -on-paper optoelectronics: drawing photodetectors with van der Waals semiconductors beyond graphite, Nanoscale 12 (2020) 19068–19074, https://doi.org/10.1039/D0NR02268C
[16] M. Lee, A. Mazaheri, H.S.J. van der Zant, R. Frisenda, A. Castellanos-Gomez, Drawing WS 2 thermal sensors on paper substrates, Nanoscale 12 (2020) 22091–22096, https://doi.org/10.1039/D0NR06036D
[17] W. Zhang, Q. Zhao, C. Munuera, M. Lee, E. Flores, J.E.F. Rodrigues, J.R. Ares, C. Sanchez, J. Gainza, H.S.J. van der Zant, J.A. Alonso, I.J. Ferrer, T. Wang, R. Frisenda, A. Castellanos-Gomez, Integrating van der Waals materials on paper substrates for electrical and optical applications, Appl. Mater. Today 23 (2021) 101012, https://doi.org/10.1016/j.apmt.2021.101012
[18] J. Azpeitia, R. Frisenda, M. Lee, D. Bouwmeester, W. Zhang, F. Mompean, H.S.J. van der Zant, M. García-Hernández, A. Castellanos-Gomez, Integrating superconducting van der Waals materials on paper substrates, Mater. Adv. 2 (2021) 3274–3281, https://doi.org/10.1039/D1MA00118C
[19] M.C. Sousa, J.W. Buchanan, Observational models of graphite pencil materials, Comput. Graph. Forum 19 (2000) 27–49, https://doi.org/10.1111/1467-8659.00386
[20] F. Carrascoso, H. Li, R. Frisenda, A. Castellanos-Gomez, Strain engineering in single-, bi- and tri-layer MoS2, MoSe2, WS2 and WSe2, Nano Res. 14 (2020) 1698–1703, https://doi.org/10.1007/s12274-020-2918-2
[21] C.-W. Lin, Z. Zhao, J. Kim, J. Huang, Pencil drawn strain gauges and chemiresistors on paper, Sci. Rep. 4 (2014) 3812.
[22] Z. Zhu, H. Zhang, K. Xia, Z. Xu, Pencil-on-paper strain sensor for flexible vertical interconnection, Microsyst. Technol. 24 (2018) 3499–3502.
[23] J. Quereda, A. Castellanos-Gomez, N. Agraït, G. Rubio-Bollinger, Single-layer MoS 2 roughness and sliding friction quenching by interaction with atomically flat substrates, Appl. Phys. Lett. 105 (2014) 053111–053142, https://doi.org/10.1063/1.4892650
[24] C. Lee, Q. Li, W. Kalb, X.Z. Liu, H. Berger, R.W. Carpick, J. Hone, Frictional characteristics of atomically thin sheets, Science 328 (80) (2010) 76–80, https://doi.org/10.1126/science.1184167
[25] A. Russo, B.Y. Ahn, J.J. Adams, E.B. Duoss, J.T. Bernhard, J.A. Lewis, Pen-on-paper flexible electronics, Adv. Mater. 23 (2011) 3426–3430, https://doi.org/10.1002/adma.201101328
[26] V. Selamneni, A. B S, P. Sahatiya, Highly air-stabilized black phosphorus on disposable paper substrate as a tunnelling effect-based highly sensitive piezoresistive strain sensor, Med. Devices Sens. 3 (2020) 800, https://doi.org/10.1002/mds3.10099
[27] H. liu, H. Jiang, F. Du, D. Zhang, Z. Li, H. Zhou, Flexible and degradable paper-based strain sensor with low cost, ACS Sustain. Chem. Eng. 5 (2017) 10538–10543, https://doi.org/10.1021/acssuschemeng.7b02540
[28] D.-J. Lee, D.Y. Kim, Paper-based, hand-painted strain sensor based on ITO nanoparticle channels for human motion monitoring, IEEE Access 7 (2019) 77200–77207, https://doi.org/10.1109/ACCESS.2019.2920920
[29] X. Liao, Z. Zhang, Q. Liao, Q. Liang, Y. Ou, M. Xu, M. Li, G. Zhang, Y. Zhang, Flexible and printable paper-based strain sensors for wearable and large-area green electronics, Nanoscale 8 (2016) 13025–13032, https://doi.org/10.1039/C6NR02172G
[30] C. Casiraghi, M. Macucci, K. Parvez, R. Worsley, Y. Shin, F. Bronte, C. Borri, M. Paggi, G. Fiori, Inkjet printed 2D-crystal based strain gauges on paper, Carbon N. Y 129 (2018) 462–467, https://doi.org/10.1016/j.carbon.2017.12.030
[31] T.-K. Kang, Tunable piezoresistive sensors based on pencil-on-paper, Appl. Phys. Lett. 104 (2014) 073117–073142, https://doi.org/10.1063/1.4866440
[32] X. Liao, Q. Liao, X. Yan, Q. Liang, H. Si, M. Li, H. Wu, S. Cao, Y. Zhang, Flexible and highly sensitive strain sensors fabricated by pencil drawn for wearable monitor, Adv. Funct. Mater. 25 (2015) 2395–2401, https://doi.org/10.1002/adfm.201500094
[33] W. Zhang, Q. Zhao, S. Puebla, T. Wang, R. Frisenda, A. Castellanos-Gomez, Optical microscopy–based thickness estimation in thin GaSe flakes, Mater. Today Adv. 10 (2021) 100143, https://doi.org/10.1016/j.mtadv.2021.100143
[34] Q. Hua, H. Liu, J. Zhao, D. Peng, X. Yang, L. Gu, C. Pan, Bioinspired electronic whisker arrays by pencil-drawn paper for adaptive tactile sensing, Adv. Electron. Mater. 2 (2016) 800, https://doi.org/10.1002/aelm.201600093
[35] Q. Li, H. Liu, S. Zhang, D. Zhang, X. Liu, Y. He, L. Mi, J. Zhang, C. Liu, C. Shen, Z. Guo, Superhydrophobic electrically conductive paper for ultrasensitive strain sensor with excellent anticorrosion and self-cleaning property, ACS Appl. Mater. Interfaces 11 (2019) 21904–21914, https://doi.org/10.1021/acsami.9b03421
[36] Y. Long, P. He, R. Xu, T. Hayasaka, Z. Shao, J. Zhong, L. Lin, Molybdenum-carbide-graphene composites for paper-based strain and acoustic pressure sensors, Carbon N. Y 157 (2020) 594–601, https://doi.org/10.1016/j.carbon.2019.10.083
[37] B. Saha, S. Baek, J. Lee, Highly sensitive bendable and foldable paper sensors based on reduced graphene oxide, ACS Appl. Mater. Interfaces 9 (2017) 4658–4666, https://doi.org/10.1021/acsami.6b10484
[38] H. Liu, H. Xiang, Y. Ma, Z. Li, Q. Meng, H. Jiang, H. Wu, P. Li, H. Zhou, W. Huang, Flexible, degradable, and cost-effective strain sensor fabricated by a scalable papermaking procedure, ACS Sustain. Chem. Eng. 6 (2018) 15749–15755, https://doi.org/10.1021/acssuschemeng.8b04298
[39] X. Qi, X. Li, H. Jo, K. Sideeq Bhat, S. Kim, J. An, J.-W. Kang, S. Lim, Mulberry paper-based graphene strain sensor for wearable electronics with high mechanical strength, Sens. Actuators A Phys. 301 (2020) 111697, https://doi.org/10.1016/j.sna.2019.111697
[40] Y. Li, Y.A. Samad, T. Taha, G. Cai, S.Y. Fu, K. Liao, Highly flexible strain sensor from tissue paper for wearable electronics, ACS Sustain. Chem. Eng. 4 (2016) 4288–4295, https://doi.org/10.1021/acssuschemeng.6b00783
[41] S. Chen, Y. Song, D. Ding, Z. Ling, F. Xu, Flexible and anisotropic strain sensor based on carbonized crepe paper with aligned cellulose fibers, Adv. Funct. Mater. 28 (2018) 800, https://doi.org/10.1002/adfm.201802547
[42] J. Luo, Y. Yao, X. Duan, T. Liu, Force and humidity dual sensors fabricated by laser writing on polyimide/paper bilayer structure for pulse and respiration monitoring, J. Mater. Chem. C 6 (2018) 4727–4736, https://doi.org/10.1039/c8tc00457a
[43] X. Liao, Z. Zhang, Q. Liang, Q. Liao, Y. Zhang, Flexible, cuttable, and self-waterproof bending strain sensors using microcracked gold nanofilms@paper substrate, ACS Appl. Mater. Interfaces 9 (2017) 4151–4158, https://doi.org/10.1021/acsami.6b12991
[44] S. Chun, Y. Choi, W. Park, All-graphene strain sensor on soft substrate, Carbon N. Y 116 (2017) 753–759, https://doi.org/10.1016/j.carbon.2017.02.058
[45] H.Y. Qi, W.T. Mi, H.M. Zhao, T. Xue, Y. Yang, T.L. Ren, A large-scale spray casting deposition method of WS2 films for high-sensitive, flexible and transparent sensor, Mater. Lett. 201 (2017) 161–164, https://doi.org/10.1016/j.matlet.2017.04.062

Dr. Andres Castellanos-Gomez is a Research Scientist in the Spanish National Research Council (Consejo Superior de Investigaciones Científicas, CSIC). He explores novel 2D materials and studies their mechanical, electrical and optical properties with special interest on the application of these materials in nanomechanical and optoelectronic devices. Among other recognitions has been appointed Fellow of the International Association of Advanced Materials (IAAM) in 2020, has been included in the Highly Cited Researchers 2018, 2019 and 2020 lists of Clarivate/WOS and has been also recognized with the Young Researcher Award (experimental physics) of the Royal Physical Society of Spain (2016).